Science Advances

AAAS

advances.sciencemag.org/cgi/content/full/4/5/eaar4418/DC1

# Supplementary Materials for

## Gold nanocrystal labels provide a sequence–to–3D structure map in SAXS reconstructions

Thomas Zettl, Rebecca S. Mathew, Xuesong Shi, Sebastian Doniach, Daniel Herschlag, Pehr A. B. Harbury, Jan Lipfert

Published 25 May 2018, *Sci. Adv.* **4**, eaar4418 (2018)
DOI: 10.1126/sciadv.aar4418

**This PDF file includes:**

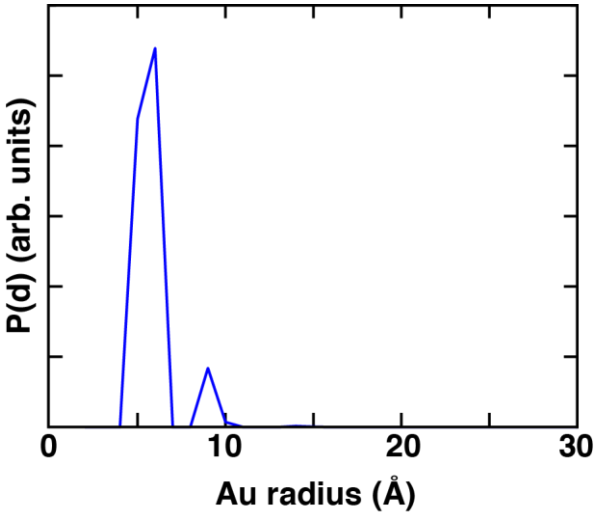


**fig. S1. Radius distribution of gold nanocrystals. (**Volume-weighted) radius distribution of a typical gold nanocrystal batch determined from SAXS (see Methods). The nanoparticles are monodisperse with a radius centered at 6-7 Å.

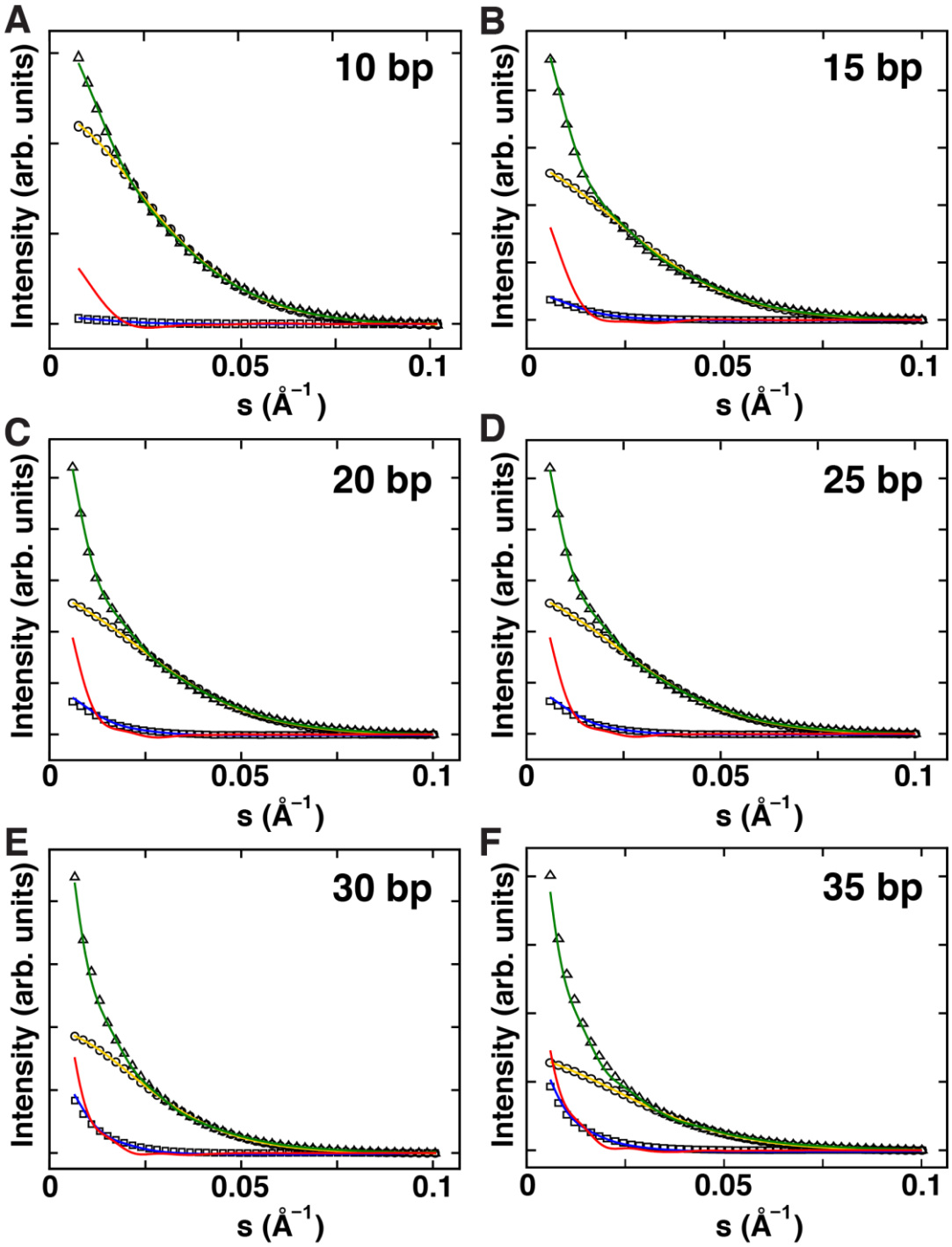


**fig. S2. SAXS scattering profiles of end-labeled DNA samples for label position reconstruction.** The panels show experimental and reconstructed data for **(A)** 10 bp, **(B)** 15 bp, **(C)** 20 bp, **(D)** 25 bp, **(E)** 30 bp and **(F)** 35 bp DNA. Experimentally measured profiles of single labeled molecules (black triangles), gold nanocrystals in solution (black circles), and unlabeled DNA molecules (black squares) are displayed in each panel. The number of *s*-bins shown was reduced for clarity. Reconstructed profiles of single labeled DNA (green line), gold nanocrystals in solution (yellow line), unlabeled DNA (blue line) and the cross scattering term between gold nanocrystal and molecule (red line) are shown in each panel. The intensity ratio at low s values between unlabeled molecule and gold nanocrystal is clearly decreasing with higher molecular mass of the molecule (from (A) to (F)).

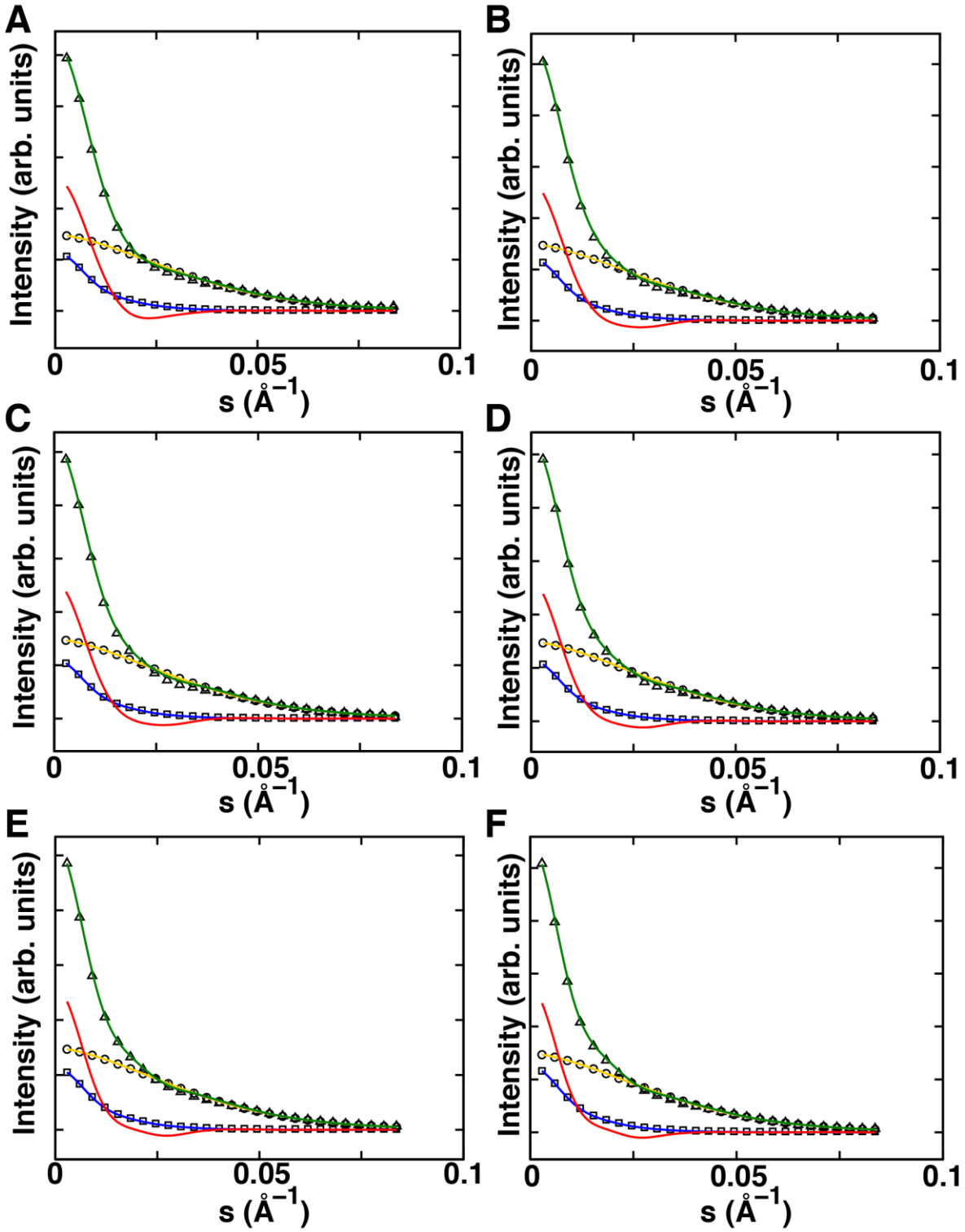


**fig. S3. SAXS scattering profiles of the full set of DNA samples for internal label position reconstruction.** The panels show experimental and reconstructed data for **(A)** B11, **(B)** B17, **(C)** A8, **(D)** A19, **(E)** A21 and **(F)** A4 DNA (see main text and table S2). Experimentally measured profiles of single labeled molecules (black triangles), gold nanocrystals in solution (black circles), and unlabeled DNA molecules (black squares) are displayed in each panel. The number of *s*-bins shown was reduced for clarity. Reconstructed profiles of single labeled DNA (green line), gold nanocrystals in solution (yellow line), unlabeled DNA (blue line) and the cross-scattering term between gold nanocrystal and molecule (red line) are shown in each panel.

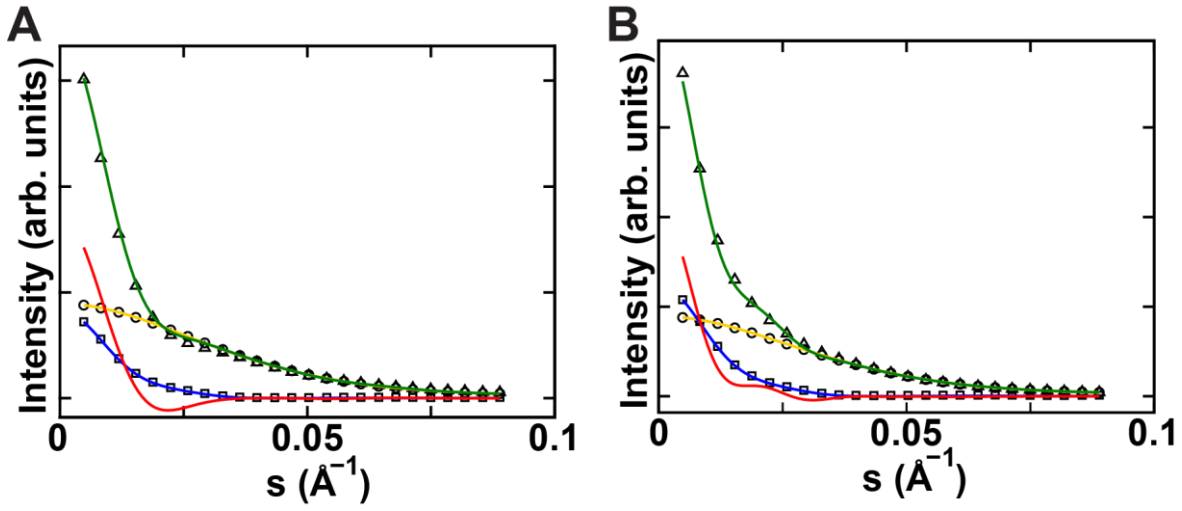


**fig. S4. SAXS scattering profiles of two end-labeled RNA kink-turn motif samples.** The shown panels contain experimental and reconstructed data for **(A)** A-strand and **(B)** B-strand labeled constructs. Experimentally measured profiles of single labeled molecules (black triangles), gold nanocrystals in solution (black circles), and unlabeled DNA molecules (black squares) are displayed in each panel. The number of *s*-bins shown was reduced for clarity. Reconstructed profiles of single labeled RNA (green line), gold nanocrystals in solution (yellow line), unlabeled RNA (blue line) and the cross scattering term between gold nanocrystal and molecule (red line) are shown in each panel.

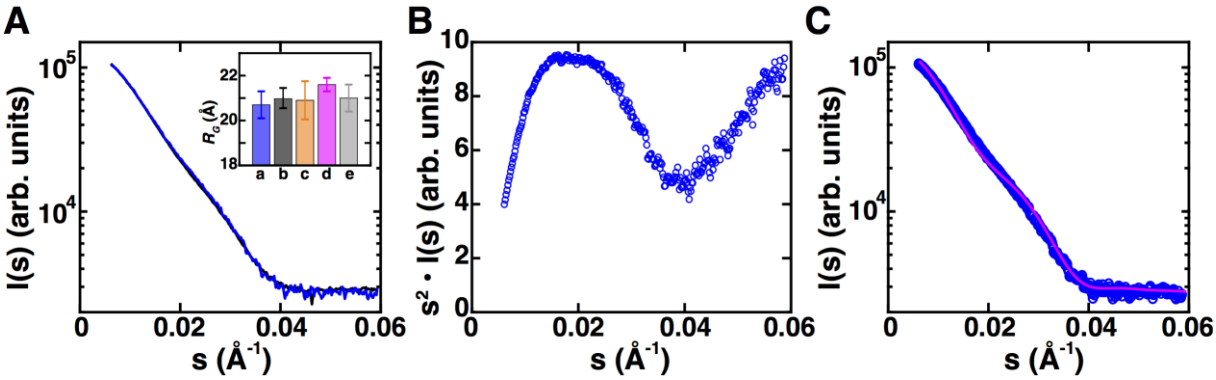


**fig. S5. SAXS data for unlabeled calmodulin. (A)** Comparison of experimental scatter profiles for calmodulin recorded in the presence of 5 mM $CaCl_2$ (blue) or 10 mM $CaCl_2$ (black). The inset shows the radii of gyration $R_G$ from different sets of experimental data in the presence of $Ca^{2+}$. Data sets are: (a): This work, 5 mM $CaCl_2$ (blue); (b): This work, 10 mM $CaCl_2$ (black); (c): Seaton *et al.* (*34*) (orange); (d): Kataoka *et al.* (*38*) (magenta); (e): Heidorn and Trewhella (*37*) (grey). $R_G$ values and errors were calculated in this work via Guinier analysis using Primus (*53*). Errors for literature values were estimated calculating the standard deviation between values given for Guinier analysis and extrapolation to zero concentration (orange, grey) or Guiner analysis and indirect Fourier transformation (magenta). **(B)** Kratky plot of calmodulin scattering data recorded in the presence of 5 mM $CaCl_2$. **(C)** Experimental scattering data of calmodulin (blue circles) and scattering profile predicted from a crystal structure of a homologous (~90% sequence identity) calmodulin using FoXS (*40*) (magenta line; PDB code: 1EXR (*27*)).

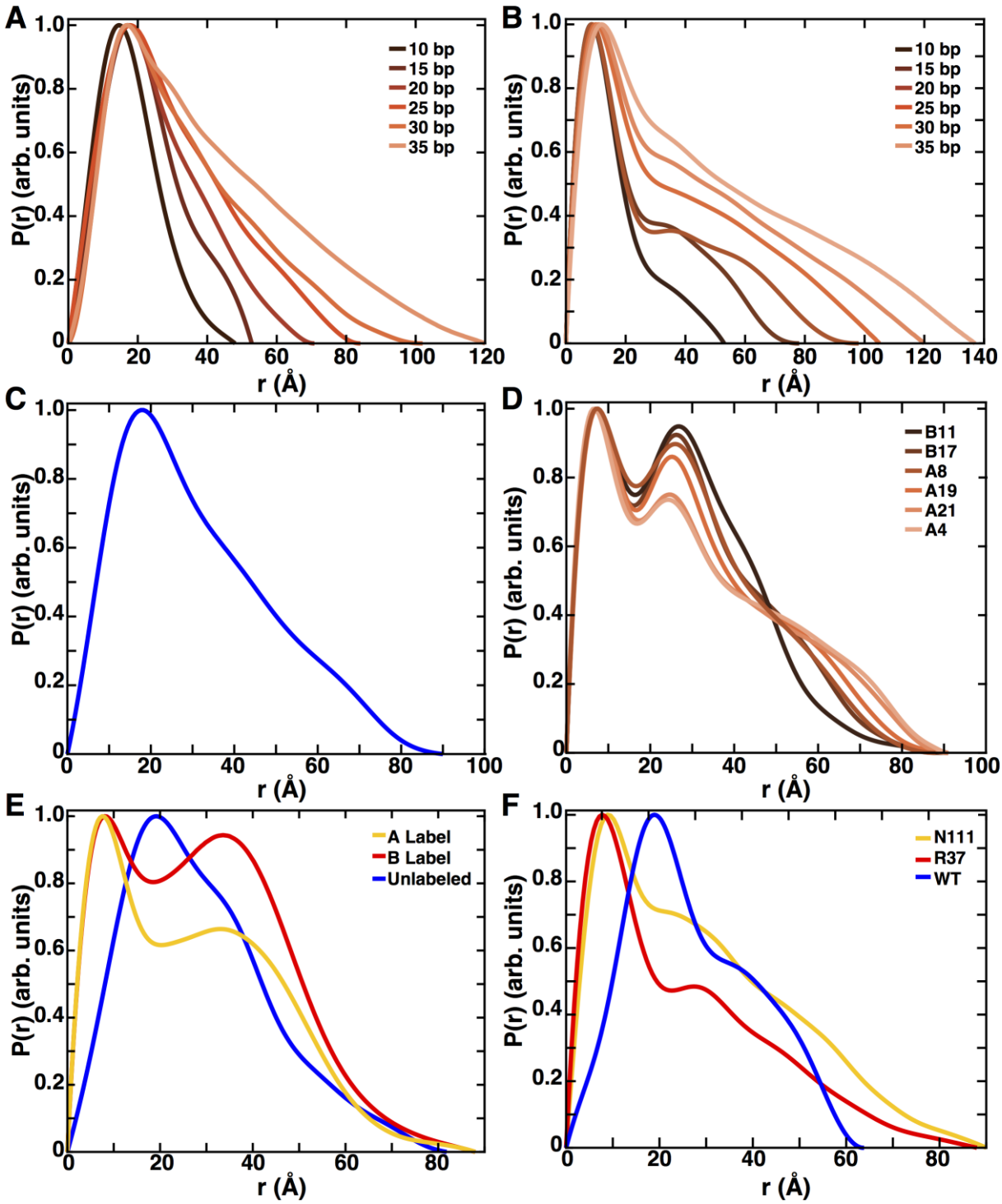


**fig. S6. Pair-distance distributions for all unlabeled and labeled samples. (A)** Pair-distance distributions for unlabeled DNA from 10 bp to 35 bp. **(B)** Pair-distance distributions for end-labeled DNA from 10 bp to 35 bp. **(C)** Pair-distance distribution for unlabeled 26 bp DNA. **(D)** Pair-distance distributions for internal labeled 26 bp DNA. **(E)** Pair-distance distributions for the unlabeled RNA kink-turn (blue), the labeled A strand (dark yellow) and the labeled B strand (red). **(F)** Pair-distance distributions for the unlabeled wildtype of calmodulin (blue), the N111C (dark yellow) labeled and R37C (red) labeled construct. The pair-distance distributions were calculated using Primus (*53*) and normalized by dividing by the maximum value in the distribution.

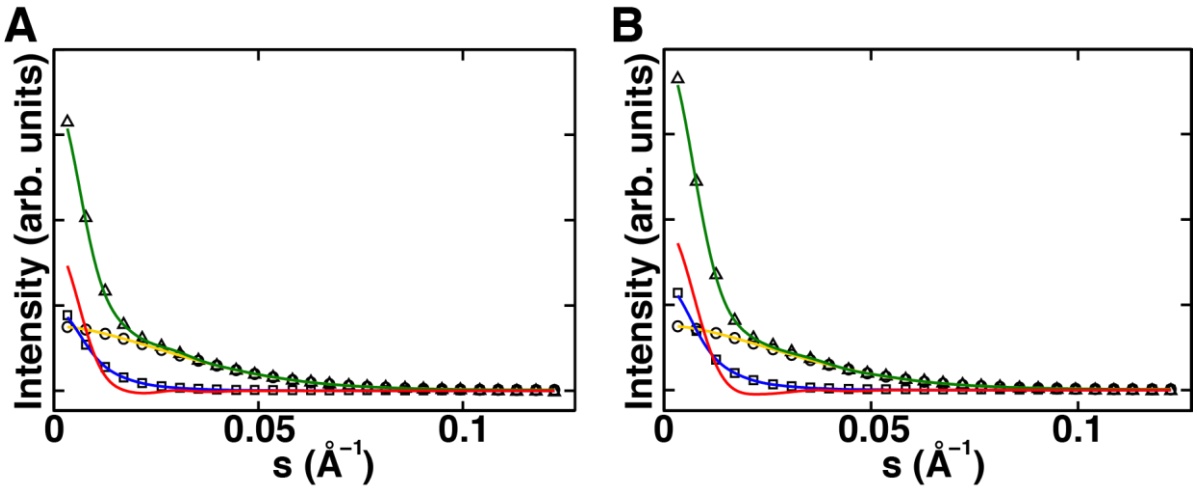


**fig. S7. SAXS scattering profiles of two different labeled calmodulin samples.** The panels show experimental and reconstructed data for calmodulin mutants **(A)** N111C and **(B)** R37C. Experimentally measured profiles of single labeled molecules (black triangles), gold nanocrystals in solution (black circles), and unlabeled DNA molecules (black squares) are displayed in each panel. Measured data sets were reduced for clarity. Reconstructed profiles of single labeled DNA (green line), gold nanocrystals in solution (yellow line), unlabeled DNA (blue line) and the cross scattering term between gold nanocrystal and molecule (red line) are shown in each panel as solid lines.

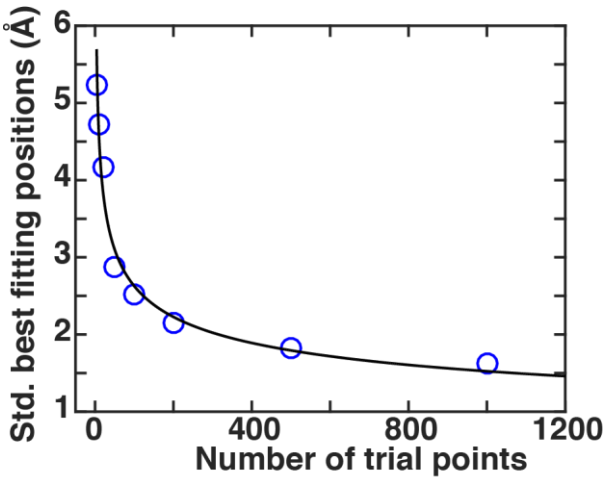


**fig. S8. Spread of the best-fitting position depending on the initial trial point density.** Sets from 5 to 1000 initial trial points per bead in the reconstructed molecular density map were created for one exemplary internally-labeled 26 bp DNA construct. The best fitting positions were calculated and the standard deviation along the helical axis (see Results) was calculated for the best 100 fitting positions. The black line is a fit of a one-component exponential equation.

**table S1. DNA sequences used in the experiments on end-labeled DNA.**

| DNA construct | Sequence |
|---|---|
| 10 bp | 5'-GCATCTGGGC-3'<br>CGTAGACCCG |
| 15 bp | 5-CGACTCTACGGAAGG-3'<br>GCTGAGATGCCTTCC |
| 20 bp | 5'-CGACTCTACGGCATCTGCGC-3'<br>GCTGAGATGCCGTAGACGCG |
| 25 bp | 5'-CGACTCTACGGAAGGGCATCTGCGC-3'<br>GCTGAGATGCCTTCCCGTAGACGCG |
| 30 bp | 5'-CGACTCTACGGAAGGTCTCGGACTACGCGC-3'<br>GCTGAGATGCCTTCCAGAGCCTGATGCGCG |
| 35 bp | 5'-CGACTCTACGGAAGGGCATCTCTCGGACTACGCGC-3'<br>GCTGAGATGCCTTCCCGTAGAGAGCCTGATGCGCG |

**table S2. DNA sequences used in the experiments with internally labeled DNA.** The bases labeled in red font denote the modified position for the gold nanocrystal attachment. Sequences for strands A are shown on top, for strand B on bottom.

| DNA construct | Sequence |
|---|---|
| 26 bp<br>A4 - internal | 5'-CGATCCGTGAAGGCGATCTCTGCGGC-3'<br>GCTAGGCACTTCCGCTAGAGACGCCG |
| 26 bp<br>A8 - internal | 5'-CGATCCGTGAAGGCGATCTCTGCGGC-3'<br>GCTAGGCACTTCCGCTAGAGACGCCG |
| 26 bp<br>A19 - internal | 5'-CGATCCGTGAAGGCGATCTCTGCGGC-3'<br>GCTAGGCACTTCCGCTAGAGACGCCG |
| 26 bp<br>A21 - internal | 5'-CGATCCGTGAAGGCGATCTCTGCGGC-3'<br>GCTAGGCACTTCCGCTAGAGACGCCG |
| 26 bp<br>B11 - internal | 5'-CGATCCGTGAAGGCGATCTCTGCGGC-3'<br>GCTAGGCACTTCCGCTAGAGACGCCG |
| 26 bp<br>B17 - internal | 5'-CGATCCGTGAAGGCGATCTCTGCGGC-3'<br>GCTAGGCACTTCCGCTAGAGACGCCG |

**table S3. RNA kink-turn sequence. Sequences for strands A are shown on top, for strand B on bottom.**

| RNA construct | Sequence |
|---|---|
| 27 bp | 5'-GCUCUCUCCAGCGAAGAACUUGGUUGC-3'<br>CGAGAGAGGUCG - - - AGGGAACCAACG |

**table S4. Radii of gyration $R_g$ values for all unlabeled and labeled samples.** The radius of gyration values were calculated from Guinier analysis using Primus (*53*).

| **Sample:** | **Radius of gyration $R_g$ (Å):** |
|---|---|
| 10 bp unlabeled | 14.0 ± 0.2 |
| 10 bp labeled | 11.7 ± 0.1 |
| 15 bp unlabeled | 17.6 ± 0.3 |
| 15 bp labeled | 17.5 ± 0.3 |
| 20 bp unlabeled | 19.8 ± 0.4 |
| 20 bp labeled | 21.1 ± 0.5 |
| 25 bp unlabeled | 21.6 ± 1.3 |
| 25 bp labeled | 18.5 ± 0.6 |
| 30 bp unlabeled | 24.3 ± 2.4 |
| 30 bp labeled | 24.2 ± 2.4 |
| 35 bp unlabeled | 28.6 ± 2.3 |
| 35 bp labeled | 26.9 ± 1.4 |
| | |
| 26 bp unlabeled | 24.7 ± 0.4 |
| B11 internal label | 21.0 ± 0.3 |
| B17 internal label | 22.0 ± 0.3 |
| A8 internal label | 21.9 ± 0.3 |
| A19 internal label | 22.8 ± 0.3 |
| A21 internal label | 23.7 ± 0.4 |
| A4 internal label | 24.2 ± 0.4 |
| | |
| RNA kink-turn unlabeled | 27.9 ± 0.7 |
| RNA kink-turn A label | 24.2 ± 0.5 |
| RNA kink-turn B label | 25.6 ± 0.6 |
| | |
| Calmodulin unlabeled | 20.7 ± 0.4 |
| Calmodulin R37C label | 19.8 ± 0.8 |
| Calmodulin N111C label | 23.9 ± 0.6 |